The ventral striatum in goal-directed behavior and sleep: intrinsic network dynamics, motivational information and relation with the hippocampus

Lansink, C.S.

CHAPTER 2

A split microdrive for simultaneous multi-electrode recordings from two brain areas in awake small animals

Carien S. Lansink, Mattijs Bakker, Wietze Buster, Jan Lankelma, Ruud van der Blom, Rinus Westdorp, Ruud N.J.M.A. Joosten, Bruce L. McNaughton and Cyriel M.A. Pennartz

J. Neuroscience methods (2007) 162: 129-138

Abstract

Complex cognitive operations such as memory formation and decision-making are thought to be mediated not by single, isolated brain structures but by multiple, connected brain areas. To facilitate studies on the neural communication between connected brain structures, we developed a multi-electrode microdrive for chronically recording ensembles of neurons in two different brain areas simultaneously. The 'split drive' contains 14 independently movable microdrivers that were designed to hold tetrodes and to permit day-to-day adjustment of dorsoventral position in the brain. The limited weight of the drive allowed rats to adjust well to the headstage after recovering from surgery and permitted stable recording sessions across at least several weeks. In addition to describing the design and assembly of the split drive, we also discuss some important individual parts of microdrives used for tetrode recordings in general. Furthermore, the split drive was applied to two widely separated and connected brain structures, the hippocampus and ventral striatum. From these two areas, stable ensemble recordings were conducted in rats performing a reward-searching task on a triangular track, yielding group sizes of about 15 and 25 units in the dorsal hippocampus and ventral striatum, respectively.

Introduction

To advance our understanding of the neurophysiological basis of cognitive processes such as memory, spatial navigation, decision-making and planning of complex movements, it is mandatory to conduct multi-neuron extracellular recordings from the brains of awake animals. Over the past decades there has been an increasing tendency to work with freely moving animals, particularly to study naturalistic behaviors and cognitive processing under low-restraint and low-stress conditions. Furthermore, as more investigators are realizing the need to investigate the neurophysiology of behavior and cognition at the neural-network or assembly level, research has been recently shifting from single-unit to multiple single-unit (or ensemble) recordings. This need has been fuelled by the notion that, in vertebrates, cognitive functions are likely to be mediated by networks of many interconnected neurons rather than single cells (e.g. Georgopoulos et al., 1989; Churchland and Sejnowski, 1992; Pennartz et al., 1994; Wilson and McNaughton, 1994; Laubach et al., 2000; Pouget et al., 2000; Miyashita, 2004) and thus should be addressed with methods for probing network activity. Important advances have already been made in meeting this need, particularly for ensemble recordings in smaller animals such as birds, rats and mice (O'Keefe and Recce, 1993; Wilson and McNaughton, 1993; Gothard et al., 1996; McHugh et al., 1996; Bragin et al., 2000; Fee and Leonardo, 2001; Lin et al., 2006).

In addition to this growing interest in neural network functioning in general, evidence has accumulated to suggest that complex cognitive operations involve interconnected brain structures. For instance, hippocampal-neocortical interactions are deemed necessary for long-term episodic and semantic memory formation (Squire and Zola-Morgan, 1991; Kim and Fanselow, 1992; Eichenbaum, 2000; Pennartz et al., 2002). Behavioral studies using disconnection lesions or split-brain paradigms have indicated a requirement for communication between connected brain structures for different cognitive operations, e.g. amygdala-orbitofrontal cortex interactions in control over response selection by reinforcer value (Baxter et al., 2000), prefrontal-ventral striatal interactions in affective modulation of attention and flexibility (Christakou et al., 2004), interhemispheric frontal interactions in executive control over memory retrieval (Miyashita, 2004) and frontal eye field-superior collicular interactions in oculomotor control (Hanes and Wurtz, 2001). Several methods have been developed thus far to realize high-density recordings from more than one brain area simultaneously. One such approach is to chronically implant sets of microwires remaining stationary in multiple target areas, due to being fixed to the cranium at the time of surgery (e.g. Chapin and Woodward, 1982; Nicolelis et al., 1997). Although successful, this approach does not allow one to optimize the number and quality of unit recordings from session to session and may gradually lead to signal loss due to gliosis and immunoreactions in peri-electrode tissue (Biran et al., 2005; Spataro et al., 2005). Alternatively, rigid electrode arrays for recording from neocortical regions have been used (e.g. Utah intracortical electrode array; Rousche and Normann, 1998), as well as rectangular grids ("warp drives") containing 144 75 μm-diameter, stainless steel electrodes that could be manually pushed down into brain tissue, however with limited electrode density and without the option of using tetrodes (Hoffman and McNaughton, 2002; Battaglia et al., 2004b). Joint ensemble recordings from rat hippocampus and medial prefrontal cortex (Siapas et al., 2005) and from two subregions within the hippocampus (Maurer et al., 2005) have been recently published, but the microdrive arrays used in these studies were not described in detail.

Here we present a ´split drive´ for dual-area ensemble recordings that was based on previous designs for single-area tetrode recordings (Gothard et al., 1996; Knierim et al., 2000; formerly marketed by Kopf Instruments, Tujunga CA., U.S.A.) and was designed to meet the following requirements: (i) considering the advantages of tetrodes in isolating single-units and yielding high numbers of cells (McNaughton et al., 1983a; O'Keefe and Recce, 1993; Gray et al., 1995), the drive had to be compatible with the use of this type of electrode arrangement; (ii) it had to contain independently movable drivers for optimal positioning of each tetrode; our instruments contains 14 microdrivers based on earlier

designs using lead screws (Ainsworth and O'Keefe, 1977; Wilson and McNaughton, 1993); (iii) the design should enable investigators to record from two widely separated areas in the rat brain and a deep (ventral) location of either area in the brain; (iv) fast, reliable and spatially accurate operation of each microdriver, at the same time being compatible with mild restraint of the animal during electrode displacement, and (v) limited weight (up to 30 grams in the design presented, which was validated in rats). While it appeared possible to meet these requirements, special attention will be given here to solving the problem of how to spatially configure and bend the cannulae that guide the tetrodes into two separated bundles. In addition, we describe some parts of multi-tetrode drives that have not been presented in detail before, as well as the use of the split drive for two interconnected brain areas – the hippocampus and ventral striatum of the rat – and some innovative modifications that may help further improve the utilization of tetrodes in general.

Materials and Methods

Subjects and behavioral procedures

Split microdrives were tested in four male Wistar rats (375-425 g, Harlan, the Netherlands). The animals were individually housed under a 12/12 hours light/dark cycle with light onset at 8:00 AM, recording sessions being performed in the animal's inactive (day) phase. Animals were water-restricted but had *ad libitum* access to food during shaping and recording days. Access to water in the home cage was limited to a 2-hour period following the recording and training session, added to consumption of reward during the session itself. All experiments were carried out in accordance with national guidelines on animal experimentation.

Before surgery, rats were shaped to run back and forth along a linear track to obtain reinforcements at both ends. Runs were partially reinforced with three types of reward (10% sucrose solution, vanilla desert or chocolate mousse). Following surgery and recovery, rats were first retrained on linear track running until pre-surgery performance levels were reached, and next introduced to a novel task. In this task the rat was required to search for reinforcement by running in one direction along a triangular track (length of equilateral sides, 90 cm, width 10 cm). Running was interrupted by visits to three reward wells placed at the center of each side under a partial reinforcement schedule (probability of reward was 33% per well visit). The types of reinforcement were the same as mentioned above, with each of the three reward types applied to one and the same cup. Thus, each type of reward was assigned to a fixed cup location throughout all recording sessions of a single rat. A single reward was delivered to one of the three cups during a full lap along the triangle according to a pseudorandom schedule. The triangle task, lasting about 20 min.,

was flanked by two rest periods (rest 1, 20-60 min.; rest 2, 60-120 min.). Rest episodes were spent inside a ´nest´ consisting of a towel folded into a wide flowerpot next to the triangular track.

Split microdrive design and assembly

The design of the split drive (Fig. 2.1) was derived from earlier tetrode drives as used by Wilson and McNaughton (1993) and Gothard et al. (1996). It resembled these drives in its basic inverted-cone or 'calyx' shape and the use of a circular array of drive screws to move tetrodes up and down. A drive nut was mounted on each screw, with a drive cannula holding the tetrode parallel to the drive screw. Although these nuts and screws have been used in previous studies, they have not been described in detail. Therefore we will pay some attention to these aspects in addition to the parts specific for the split microdrive.

The split drive was divided into an upper section, containing the array of 14 drive screws with attached drive nuts and cannulae, a middle section or ´core´, and a bottom section including the two bundles targeted towards the two brain areas of interest (Fig. 2.1A). The total weight, height and top diameter of the split drive amounted to about 27 g, 5.6 cm and 4.1 cm, respectively.

An example of a drive screw-nut-cannula configuration, repeated 14 times full-circle in the upper section, is shown in Fig. 2.2A. The screws were 1.6 mm in diameter, made of stainless steel (type 304), with a full turn corresponding to a vertical displacement of 350 μm. The screw was anchored into the core piece and could not rotate. The core was made of either Makrolon or Kel-F (Vink Kunststoffen, the Netherlands), a type of Teflon that is particularly resistant to chemicals and deformation. Drive nuts were made of aluminium and had two indentations of unequal width at their upper surface (Fig. 2.2E). Each nut was set in a mantle piece made of Makrolon or Lexan. Hereafter we will refer to an individual drive cannula holding a tetrode and being mounted in the mantle piece as a ´leg´. Any leg could be moved up and down manually by fitting a turn-tool onto the indented surface of the nut, with two protrusions of the turn-tool uniquely matching the indentations. When the turn-tool was thus fitted onto the nut, the nut was able to rotate around the drive screw and inside the mantle, which did not rotate itself. Legs were made of stainless steel (Small Parts, Miami Lakes, Fl., U.S.A., inner and outer diameter: 0.33 and 0.64 mm). The drive screw-nut combination was constructed to allow the nut to rotate around the drive screw, with low friction relative to the mantle piece. Besides the channel for the drive screw, the mantle piece contained two vertically oriented drill holes, one of which fitted the leg that was fixed to it by glue. The other hole fitted a solid conducting bar (stainless steel, 0.7 mm

in diameter) along which the nut and mantle piece were sliding during down- or upward movement. This construction kept the leg in the same lateral position with respect to the screw and ensured its stable, rectilinear vertical descent parallel to the screw. This effect was achieved because the conducting bar was firmly anchored into the core and kept the mantle piece in place, whereas the nut could freely rotate around the drive screw. While the nut was rotating downwards, it also drove the mantle piece along because the nut's upper and lower edges extended slightly laterally over the corresponding contours of the mantle piece (Fig. 2.2E). We refer to the parallel configuration of drive screw and nut, conducting bar and leg as a ´tripod´ (Fig. 2.2A).

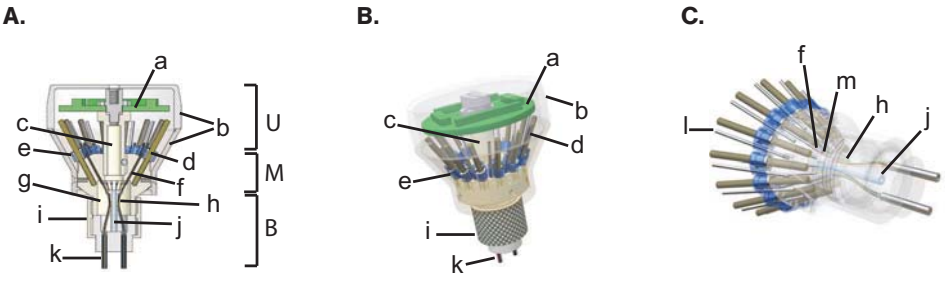

Figure 2.1

Overview of the split microdrive. (A) Longitudinal section with (a) printed circuit board, (b) dust cap and lower cover piece, (c) central post, (d) drive screw, (e) drive nut with mantle piece, (f) drive cannula or ´leg´, (g) inner cylindrical space, (h) muster place for guide cannulae, (i) screw cap, (j) element fixating guide cannulae, (k) bundle of guide cannulae held together by a casing. The total height and top width of the split microdrive were 5.6 and 4.1 cm, respectively. Upper, middle and bottom sections are indicated by U, M and B, respectively. (B) Side view of the split microdrive with the dust cover and lower cover piece rendered as transparent. The drive nuts are in the lowermost position. Lowercase characters denote the same parts as in (A). The outer surface of the screw cap was provided with a diamond-shape texture to promote attachment of dental acrylic. (C) Transparent view of the drive, showing several of its elements more clearly than in (A). A guide cannula (m) protrudes from a leg (f) and converges with other cannulae towards one of the two muster places (h). The bar for conducting the drive nut with leg up or down is represented by (l).

When drive nuts had been turned fully downwards, the attached legs protruded through the core piece via guide holes of 0.65 mm diameter. This middle section contained an inner cylindrical space (diameter: 10.0 mm; Fig. 2.1A) in which the set of legs converged into two tightly packed bundles (Fig. 2.1A and C; Fig. 2.2B and C). However, the legs holding the tetrodes throughout the upper section extended only slightly into the inner cylindrical space (1.0 mm at maximum, with tetrodes fully lowered). At this stage the legs

were sliding over a thinner type of cannula, referred to as 'guide cannula', that extended all the way down to the exit grid of the bundle (Fig. 2.1A and C; Fig. 2.2C). The spatial layout of drive cannula, guide cannula and the elements contained within these is shown in Fig. 2.3. The outer and inner diameter of the latter stainless steel cannulae were 0.31 and 0.15 mm, respectively (Advent Research Materials, Oxford, U.K.). This arrangement allowed an individual tetrode to be driven down into the brain by a vertical displacement of the leg from the upper section into the core, while the guide cannula maintained a fixed position and did not protrude into the brain, but retained its guiding function for the tetrode throughout the middle and bottom section.

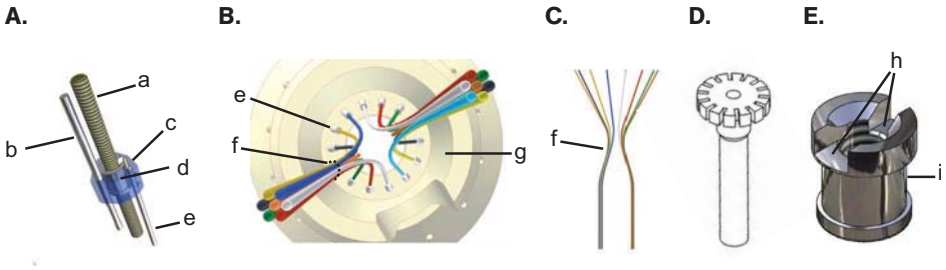

Figure 2.2

Separate renderings of important parts of the split microdrive. Note that the lowercase characters denote different parts than in Fig. 2.1. (A) Configuration of the 'tripod', consisting of (a) drive screw, (b) conducting bar, (c) mantle piece surrounding the drive nut, (d) drive nut, (e) leg. (B) Bottom view of the split drive, showing the spatial trajectory of the guide cannulae, marked by different colors for rendering purposes, as they emerge from the legs (e) and converge towards a muster place (f, indicated by dotted line). Viewpoint is located slightly below (i.e. towards the cranium) the muster places, within the inner cylindrical space. Below the muster places, the guide cannulae collectively bend away from the center towards one of the two bundles. Bottom surface of the core is indicated by (g). (C) Side view of the spatial trajectory of the guide cannulae. Tetrodes can be inferred to pass through two curves, one centered close to the muster places (f) and one at the point where the thin guide cannulae are aligned vertically to pass straight through the bundles. (D) Element fixating the guide cannulae at a point slightly above the muster places (Fig. 2.1A). This element contained 14 indentations, each holding a guide cannula in place. (E) Detailed view of the drive nut. The indentations of unequal width for fitting a turn-tool are indicated by (h). The mantle piece fitted onto the cylindrical surface denoted by (i), allowing free rotation of the nut, and did not cover the slightly wider upper- and lowermost parts of the nut.

The requirement that made the split drive especially different from a ´monodrive´ (i.e. a tetrode array with one bundle targeted towards a single brain area; Gothard et al.

1996) was that a smooth sliding movement of the legs over the guide cannulae must be combined with a divergence of the two sets of tetrodes towards the bundles (Fig. 2.1A). In the case of joint hippocampal-ventral striatal recordings, a distance of 5.8 mm between the bundle centers was required. A potential problem in this configuration is that the guide cannulae start diverging too close to the lowermost point where the legs are sliding over them. The solution chosen to avoid this problem was to construct the array of guide cannulae such that they ran straight through the core piece, ending at 2 mm above the upper core surface, whereas further down they converged to two muster places (Fig. 2.1A and C; Fig. 2.2B and C), from which they gradually diverged towards the bundles. After having entered the bundles, the downward course of the cannulae was straight again. This configuration allowed tetrodes to have a maximal vertical travel distance of 11.0 mm. To prevent buckling of the tetrodes and their supporting tubes (see below) within the guide cannulae, it was essential to achieve smooth curvatures around the muster places and points of entry into the bundles. To facilitate this, the middle and bottom sections of the split drive were made taller (+9.8 mm in total) than in the original monodrive design. The curvature around the muster places was 28° across 4.9 mm. In preliminary versions of the split drive we noted that downward movement of drive nuts and legs sometimes led to lateral excursions of the muster places, causing distortions of the curvature, which was prevented by fitting the converging cannulae through the slots of a fixating element, placed at the center of the inner cylindrical space (Fig. 2.1A, 2.2D). Application of epoxy glue onto the bottom part of the inner cylindrical space appeared also useful for this purpose. It did not prove necessary to use both a fixating element and epoxy glue. Special care was taken to approximate equal curvatures for all individual cannulae above and below the muster places. To prevent buckling during split drive assembly, cannulae were filled with music wire (0.12 mm in diameter, Small Parts) prior to bending.

The central part of the bottom section of the split drive consisted of a Kel-F piece (11.0 mm in diameter) that formed an extension of the core of the middle section and was fixed to it by a screw cap, 16.1 mm in diameter. Similarly, the inner cylindrical space of the core piece extended into the bottom part by way of a less wide space (diameter: 7.9 mm). The guide cannulae were fixated and held together in two bundles by two cylindrical stainless-steel casings, which were 9.0 mm in length and protruded below the Kel-F piece by 5 mm. The spacing between the tetrodes as they exited the hexagonal grid of each bundle amounted to 300 μm.

Tetrodes were fabricated as described before (Gray et al., 1995). Briefly, they were made by twisting together four 13-μm diameter nichrome microwires (Kanthal, Palm Coast Fl.,

U.S.A.) and forming a microbundle by melting together their polyimide coatings using a heat gun. Electrode tips were gold-plated using a gold cyanide solution (Select Plating, Meppel, Netherlands) to achieve an impedance range of 0.5 - 1.0 ΩW for tetrode wires and 0.3 - 0.4 MΩ for reference electrodes. Before the split drive could be loaded with tetrodes, we first inserted supporting tubes of fused silica (inner diameter: 65 μm, outer diameter: 127 μm; Polymicro Technologies, Phoenix Az., U.S.A.) into the legs and fixated them with glue to the top ends of the legs (Fig 2.3). Subsequently, the tetrodes were inserted into the fused silica tubes via their top ends and glued to these ends as well as the legs. The total length of the fused silica tubes was shorter than that of the tetrodes to prevent them from penetrating into brain tissue.

To relay electrical signals from the tetrode wires to the preamplifiers of the headstage, individual wires diverged from the same end points towards a custom-made printed circuit board that was held in place by a centrally positioned post, made of Kel-F (Fig.1). Gold pins or cactus needles were used to fixate microwires in each designated receptacle hole of the board, while wire insulation was locally removed by the friction caused by thrusting the pin into the hole. Low-impedance connection between tetrode tip and corresponding board output was repeatedly checked, as well as possible cross-talk between different leads. Entry of dust onto the printed circuit board or tetrode array was prevented by a plastic, semi-transparent dust cap and cover piece (Fig. 2.1A).

Surgery and tetrode positioning

Following anesthesia with 0.08 ml/100 g body weight Hypnorm i.m. (0.2 mg/ml fentanyl and 10mg/ml fluanison; Janssen Pharmaceutics, Beerse, Belgium) and 0.04 ml/100 g Dormicum s.c. (1.0 mg/kg midazolam; Roche Netherlands, Woerden), rats were mounted in a Kopf stereotaxic frame with bregma and lambda in the horizontal plane. Craniotomies, both in the right hemisphere and 1.5 mm in diameter, were made above the dorsal hippocampus (4.1 mm posterior and 2.5 mm lateral to bregma) and ventral striatum (+1.8 mm and 1.4 mm; Paxinos and Watson, 1986). After removing the dura, tetrode bundles were placed on the cortical surface and subsequently the cortical surface was covered with a viscose layer of a biocompatible, dual-component Silastic (i.e., a silicone elastomere, World Precision Instruments, Berlin, Germany). The split drive was fixed to the skull using dental cement and 6-8 small bone screws, one of which was used as ground. A few hours after surgery, pain relief was provided by applying 0.5 mg/ 100 g body weight Fynadine s.c. (flunixinum, Schering-Plough Santé Animal, Segre, France). In addition, dehydration was counteracted by postsurgical i.p. injection of at least 2.0 ml saline solution.

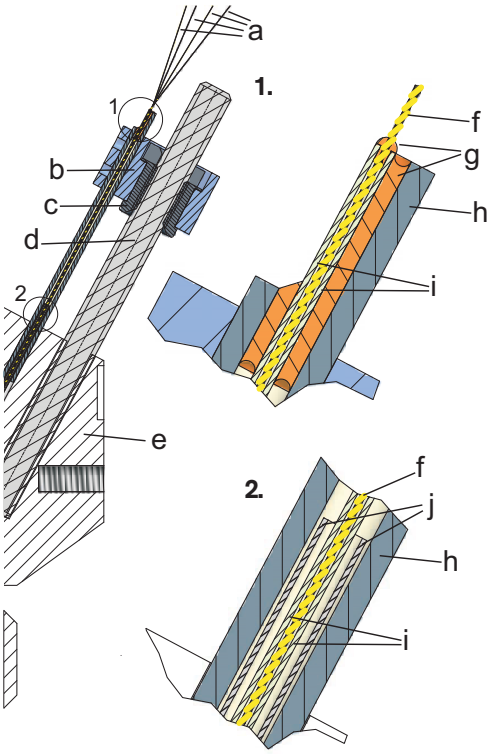

Figure 2.3

Spatial arrangement of drive nut, mantle, tetrode and other elements inside the drive cannula. The left-hand part of the figure shows a partial cross-section of the hyperdrive (cf. Fig. 2.1A) whereas the right-hand insets 1 and 2 represent enlargements of the encircled regions in the left-hand overview. The overview shows how the drive cannula containing the tetrode, the individual wires of which are indicated by (a), is positioned within the mantle piece (b) mounted on the drive nut (c). During turning the drive nut rotates around the drive screw and within the mantle piece, which does not rotate but travels downward parallel to the drive screw. The drive screw and core piece are indicated by (d) and (e), respectively. Inset 1 shows how the tetrode (f, purple-yellow) is inserted into the fused silica tube (i, light green) and how these parts are positioned relative to the drive cannula or 'leg' (h, grey-blue). The tetrode and fused silica were glued to the drive cannula at the locations approximately indicated by orange patches (g). Inset 2 zooms in on the part of the drive cannula into which the guide cannula (j, light purple) is protruding. Parts common to both insets are indicated by the same characters. For rendering purposes, the relative diameters of the drive cannula, guide cannula, fused silica tube and tetrode have only been crudely approximated.

Tetrodes were lowered towards the target structures across about 7 days, including the day of surgery. Five tetrodes were targeted towards the pyramidal cell layer of hippocampal area CA1, using the dense firing activity and high-amplitude spikes in neocortical layer V, as well as the gradual increase in sharp-wave and ripple activity just dorsal of CA1's pyramidal cell layer as electrophysiological beacons. Seven tetrodes were advanced towards the ventral striatum, using layer V unit activity and the lack of such activity in the corpus callosum as guiding cues. Movement of individual tetrodes was verified by noting loss of previously recorded units and appearance of new ones, and the amounts of consecutive movement across recording sessions (usually 20-40 μm per day) were documented in a lab journal.

Following downward movement, tetrodes were left in place for at least 90 minutes before commencing recordings. A single electrode was placed in the corpus callosum above the hippocampus, serving as reference for differential recordings, and a second electrode was positioned in the hippocampal fissure for recording theta oscillations. In two out of four rats an additional reference electrode for ventral striatal recordings was placed in the corpus callosum overlying the striatum. No marked differences in noise rejection or local field potential profiles were noted when using these different reference electrodes.

Recording, data acquisition and analysis

The printed circuit board situated on top of the split drive was connected to a headstage containing 54 unity-gain field effect transistor preamplifiers (Neuralynx, Tucson, AZ, U.S.A.). Their output was relayed via flexible, multiwire cables to a 64-channel commutator with torque sensor and motor drive (Model MDC 900; Dragonfly, Ridgeley, W-Virginia, U.S.A.) and fed into eight 8-channel amplifiers (Neuralynx; amplification: 5000X; band-pass filtering: 0.6 – 6.0 kHz for single-units; local field potentials were amplified 1000X and filtered between 1 - 475 Hz). Spike waveforms passing a pre-set threshold were digitized at 32 kHz across 1 ms using a Cheetah analogue-to-digital converter (ADC) interface (Neuralynx), whereas local field potentials were sampled at 1690 Hz. The headstage contained an array of light-emitting diodes which allowed video-tracking of the rat's head position, using a camera situated about 1.5 m above the behavioral setup. The spatial and temporal resolution of the videotracking system were 2.5 mm/pixel and 16.7 ms (i.e., 1/60 Hz^{-1}), respectively. In addition, the behavior of all rats was recorded on analogue videotape for off-line analysis.

Based on their waveforms, spikes were sorted using a semi-automated clustering algorithm (BubbleClust, P. Lipa, Univ. of Arizona, Tucson, AZ, U.S.A.) and subsequently refined by visual inspection using the MClust program (A.D. Redish, Univ. of Minnesota, Minneapolis, MN, U.S.A.). In addition to the waveform characteristics recorded on the four leads of each tetrode, spike interval distributions and autocorrelograms were used to check whether clusters of spikes were attributable to a single unit. Units were not included in further analysis when firing less than 20 spikes in at least one of the three episodes. Rate maps, i.e. graphs displaying a single unit's firing rate as a function of the spatial position of the rat's head on the triangular track, were constructed by dividing up the track in spatial bins 0.75 cm in width, counting the rat's occupancy time and number of spikes that could be allocated to each bin based on the time stamps of spikes and head positions, and dividing the spike count by the occupancy time. Bins with very low occupancy ($<$ 0.167 s across the total behavioral period) were not assigned a primary firing rate value. A secondary, final firing rate value for each bin was obtained by a spatial smoothing procedure in which each

bin's primary firing rate value was averaged with the primary values from its four direct neighboring bins.

Final end positions of tetrodes were marked by passing a 25 μA current of positive polarity for 10 s through one of the four leads of each tetrode to produce a small lesion. On the next day animals were transcardially perfused (0.9 % NaCl solution followed by 4% paraformaldehyde in 0.1 M, pH 7.4 phosphate-buffered saline). Their brains were removed and cut in coronal sections (40 μm) using a Vibratome (Leica, type VT-1000S, Wetzlar, Germany) and Nissl-stained.

Results

A total of 4 rats were fitted with a split microdrive; they all adapted to carrying the split hyperdrive on their heads within a few days after surgery and their recovery rate was similar to rats carrying a classical monodrive. After tetrodes had been moved down to their respective target locations in the dorsal parts of the ventral striatum and dorsal hippocampus (Fig. 2.4), a total of 30 recording sessions were performed (7.5 ± 0.9, mean ± sem, per rat), yielding an average of 25.4 ± 2.1 single units per session in the ventral striatum and 14.9 ± 1.9 single units in the hippocampus. Decisions to terminate recording sessions in a given rat were mainly motivated by reaching the ventralmost position of the 7 tetrodes considered to be within the confines of the ventral striatum according to stereotaxic estimates. Thus, the current study did not assess the longevity of stable split drive implantations across many weeks or months per se, but this longevity stretched at least across the first 3-4 weeks following surgery. Proper translocation of tetrodes was confirmed by comparing their histologically identified end points with the stereotaxic coordinates calculated from the sum of distances traveled across sessions. Only rarely we failed to observe loss of recorded single units and appearance of new ones when drive screws were turned, corresponding in the histological assessment to a lesion site that was far too dorsal than stereotaxically calculated. Such ´stuck´ tetrodes can sometimes also be encountered in classical (monodrive) configurations (Gothard et al., 1996; Pennartz et al., 2004) and their rate of occurrence in split microdrives was about as low as in monodrive recordings done in our lab under similar conditions. A block of movement was observed for only 2 tetrodes (one hippocampal, one ventral striatal) across all four rats studied. Judging by the time course of spike waveform measures such as amplitude or area, unit recordings were stable across the entire session, spanning about 2 to 3 hours from the beginning to the end of the rest periods flanking the behavioral task. Thus, the sets of legs and guide cannulae can be concluded to have functioned properly, at least to the extent that a very high percentage of tetrodes could be displaced smoothly and reliably to and within the target areas across many sessions.

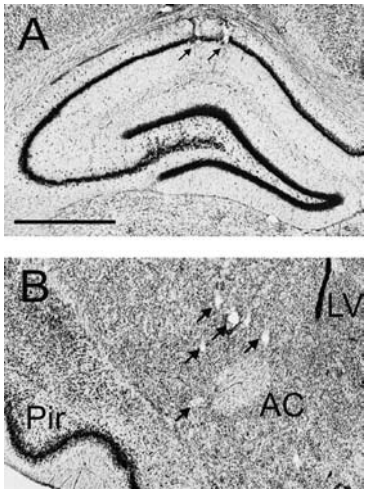

Figure 2.4

Histological assessment of electrode positions in (A) the dorsal hippocampus and (B) the ventral striatum. Both photographs represent coronal, Nissl-stained sections and were obtained from the same rat. While the tetrode tracks in area CA1 show characteristics of gliosis due to lesion currents and thus indicate end points, the lesions in the ventral striatum represent passing tracks. LV, lateral ventricle; AC, anterior commissure; Pir, piriform cortex.

Figure 2.5 presents some examples of spike clustering plots and average spike waveforms for ventral striatal units. To be included in our analysis, neurons had to have less than 0.1% of their spike intervals assuming values below 2.0 ms and low amounts of spike-amplitude drift on each of the four tetrode leads. As was the case for hippocampal units, we encountered many units in the ventral striatum that could only be distinguished well from nearby units on the same tetrode by taking into account spike waveform parameters recorded on more than one tetrode lead.

Figure 2.6 shows examples of rate maps of simultaneously recorded ventral striatal and hippocampal units. The detailed results of these recordings will be described elsewhere *(chapter 4)*. Briefly, each rate map represents the spatial distribution of the firing rate of an individual unit, quantified in square bins that were repetitively visited while the rat was running unidirectionally along a triangular track and collecting rewards. Qualitatively, it can be noted that, when ventral striatal units showed a significant change in firing rate on the track, the change was almost always incremental with respect to the background firing rate, and could be allocated in a large majority of cells to track sites corresponding to one or more reward locations, or to a spatial trajectory of about 10-40 cm directly leading up to one or more reward sites. Thus, if ventral striatal units showed a spatiotemporally differentiated firing profile on the track, their predominant pattern of activity was an increase in firing rate at or prior to one, two or three reward sites (Fig. 2.6B). Firing increments of hippocampal units (Fig. 2.6A) were restricted to particular locations distributed along the triangular track, including reward sites, and were thus characteristic of place fields, although their dependence on head direction was not explicitly verified in this task.

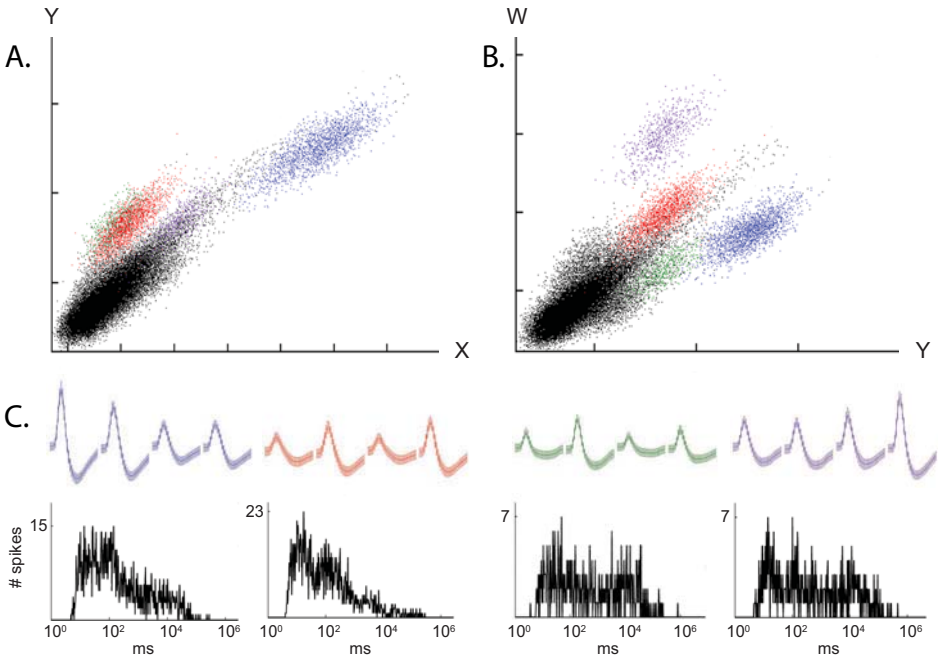

Figure 2.5

Example of spike clustering plots and spike waveforms for a tetrode recording from the ventral striatum. Spike waveform parameters such as amplitude, area, energy (i.e., sum of the squared amplitude across all 32 data points of each waveform) and principal components were used to generate the cluster plots such as shown in (A) and (B) for the same dataset recorded on a single tetrode. (A) plots the area of the spike waveform on lead X of the tetrode against lead Y of the same tetrode in arbitrary units; in (B) the same parameter is plotted for lead Y versus lead W. (C) shows averaged spike waveforms for all 4 separable clusters shown in (A) and (B) and across all leads, adopting the same color code as in (A) and (B) and plotting the waveforms on lead X, Y, Z and W from left to right for each unit. Subsequent inspection of the spike interval distributions (lower panel of C) and autocorrelograms confirmed that the clusters were attributable to single units. When in (B) the area information from the W-lead would be removed, three clusters (purple, red and green) would not be distinguishable from each other. In (A) the red and green cluster cannot be separated using both the X- and Y-leads.

Discussion

We designed a split microdrive that allowed us to simultaneously record cell assemblies in two widely separated, connected structures of the rat brain during active behavior, i.e. area CA1 of the hippocampus and the ventral striatum. To be able to continue using some drive parts that had been previously validated for single-area ensemble recordings in rats (Gothard et al., 1996), we based the design of the split drive on the original ´monodrive´ configuration.

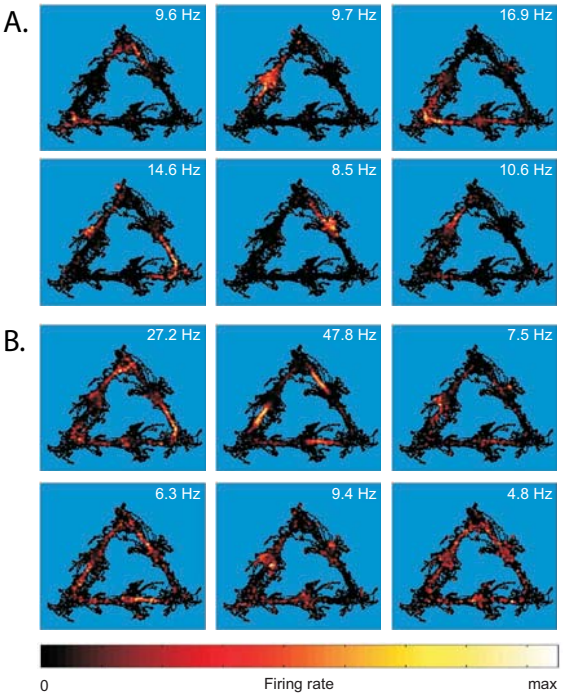

Figure 2.6

Spatial distributions of firing rate (rate maps) for simultaneously recorded hippocampal (A) and ventral striatal units (B). Based on their time stamps, each spike of each unit was attributed to a spatial bin of 0.75 cm width on the triangular track, and the color of each bin represents the local firing rate of each unit. Firing rates were color-coded according to the 'hotness' scale shown below the rate maps and ranged from 0 Hz (black) to a maximum that varied from unit to unit, as specified in the top right corner of each rate map. The exemplars shown here were part of larger hippocampal and striatal ensembles recorded with the split drive during a single session (N=15 and N=21 units, respectively). In particular, many ventral striatal units were virtually silent on the triangular track but active during rest or sleep. Units were included in the figure when they generated at least 500 spikes on the track. The running direction was clockwise. The hippocampal units in (A) showed dense firing at particular locations on the track such as in one or two corners or close to one of the three reward sites, situated in the middle of each side of the triangle. Ventral striatal units (B) exhibited firing patterns that were frequently associated with one or more reward sites and much less often with other behavioral events or locations. For example, the unit with a 47.8 Hz maximum in the middle position of the upper row in (B) showed enhanced firing when the rat approached and arrived at all three reward sites.

Major modifications were applied to the spatial trajectory of the guide cannulae and the materials used, whereas the calyx-shaped configuration of drive screws in the upper section remained virtually unchanged. Despite a modest increase in height and weight relative to a monodrive, stable ensemble firing activity from the two brain areas was recorded across behavioral sessions lasting several hours. Following surgery, the rat was well capable of adjusting to the head implant and was only mildly restrained by the attachment of a headstage and tether cables during spatial navigation. The split drive implant remained stably attached to the skull for at least several weeks, thus permitting investigators to train rats extensively on a behavioral task and perform long-lasting recording series across the complete dorsal-ventral extent of the brain areas under scrutiny. Moreover, each of

the 14 microdrivers could be operated swiftly and reliably while the rat was awake. Upon termination of an experiment, most parts of the split drive remained intact and could be used for further experiments; only tetrodes, fused silica tubes and gold pins were not reused. Occasionally, the bottom ends of the bundle and guide cannulae of hyperdrives were clogged by blood or plasma, necessitating replacement.

Although we only recorded simultaneously from hippocampus and ventral striatum in this study, the drive configuration poses no particular barriers for application to other connected brain structures. For instance, the basic split drive design can accommodate larger distances between brain areas by enlarging the bundle separation while maintaining smooth curvatures around the muster places, which may necessitate a slight increase in height of the assembly. Similarly, when target brain areas are distributed along the mediolateral axis, the bundles can be easily configured to compensate the difference in their dorsoventral cortical entry points. Brain areas which are limited in size along the anterior-posterior or mediolateral axis (e.g. medial prefrontal cortex) can be approached by producing ´flat´or ellipsoid tetrode arrangements in one or both bundles.

Whereas during tetrode descent the pyramidal cell layer of area CA1 was conventionally identified by e.g. growing sharp wave-ripple activity and exhibited firing patterns characteristic of place fields (Fig. 2.6A), unit recordings in the ventral striatum could not be distinguished from those in the dorsal striatum by particular EEG or waveform characteristics. However, their rate maps suggested an association of enhanced firing with reward locations (Fig. 2.6B) and behavior directly leading up to the acquisition of reward, which is in agreement with previous studies recording units in ventral striatum (Schultz et al., 1992; Shidara et al., 1998; Setlow et al., 2003; Pennartz et al., 2004; Roitman et al., 2005). Post-hoc histological controls confirmed that the large majority of tetrodes had reached the approximate positions predicted by day-to-day downward tetrode movements. In contrast to the assertion by Nicolelis et al. (1997) that there is no need to employ tetrodes instead of single microwires when recording from brain areas with moderate cell density, we found many ventral striatal units that were only clearly separable from other units on the same electrode lead when using spike waveform information from multiple leads (Fig. 2.5); their spikes would have been likely grouped together with those of neighboring units had only one electrode wire been available for recording. No indications were found for differences between tetrode recording quality in the split microdrive as compared to a monodrive. The numbers of units recorded per ventral striatal tetrode in our split drive were comparable with those in a previous monodrive study (Pennartz et al., 2004). Although for area CA1 a maximal cell number per tetrode of 12 or even higher has been occasionally reported (e.g.

Wilson and McNaughton, 1993), the mean and standard errors of cell numbers recorded per tetrode have not been consistently reported in the literature. Moreover, the net yield strongly depends on the criteria for accepting or rejecting spike clusters as attributable to a distinct unit.

In addition to a split drive design resembling a classical monodrive, various alternative design approaches can be adopted when aiming to record from two or more brain areas simultaneously. An alternative approach can be to manually assemble a number of tripods, held together by dental cement, which may have a certain advantage of flexibility and obviates the need for accurate micromachining facilities. However, the current split drive has the advantage of being highly reproducible and robust both in spatial layout and operation, as the tetrode array and guide cannulae can be assembled in a stereotyped manner. Successful assembly and operation does depend on the availability of micromachining facilities, which, however, do offer opportunities for upscaling of production.

In view of future multi-area ensemble recording studies, various options for expanding and enhancing multi-tetrode arrays can be envisioned. Following the introduction of a motorized, miniature 3-electrode microdrive (Fee and Leonardo, 2001), Cham et al. (2005) recently developed a semi-chronic recording system for computer-controlled positioning and signal optimization of single platinum-iridium electrodes in monkey neocortex. Motorized driving may also be applied to tetrode arrays and in other animal species such as rats, as far as weight and size remain permissive. Indeed, such motorization may reduce the time needed to search for large numbers of units in advance of each recording session, and would thus facilitate the use of larger numbers of tetrodes. A further gain in expanding the number of electrodes may be obtained by miniaturizing the microdrivers by using e.g. silicon actuators. However, the force that such small actuators can deliver requires attention, especially when vertical electrode movement is constrained by friction between electrodes and guide cannulae or brain and connective tissue.

Although in the current split drive a tetrode only rarely got ‘stuck’ because of e.g. buckling inside its guide cannula, the importance of maintaining smooth curvatures of the guide cannulae must be emphasized when aiming for expanded microdrives. For instance, sharper angles may become a problem if the distance between the two tetrode bundles were to increase markedly. Moreover, when an experiment would require multi-electrode placements in more than two brain areas, the current ‘calyx’ configuration would become less useful because of the size of the drive screw and nut, and the varying angles along which the bundles would diverge from the muster places. The technique of Hoffman and

McNaughton (2002) to record from 4 areas of the monkey neocortex simultaneously employed relatively rigid and thick single electrodes, placed in grid boards. This approach could be further enhanced by using miniature actuators for motorized electrode displacement. Alternatively, one may aim to maintain a multi-tetrode configuration for poly-areal recordings by creating multiple adjacent calyces, each directed at a different brain area, and avoiding potential problems relating to cannulae curvatures. This option should become increasingly feasible as electrode drivers and motorized actuators will be miniaturized further.

Acknowledgements

We wish to thank Peter Lipa and A. David Redish for the use of the cluster-cutting programs BubbleClust and MClust, respectively. The comments of Tobias Kalenscher, Francesco Battaglia and Jadin Jackson on the manuscript are gratefully acknowledged, as well as the contributions by Rein Visser, Theo van Lieshout and Ron Manuputy to the design and printed circuit board of the split microdrive. This work was supported by HFSPO grant RGP 0127 to BLM and CMAP, NWO-VICI grant 918.46.609, BSIK grant 03053 from SenterNovem, the Netherlands, both to CMAP and by PHS grant NS20331 to BLM.